

# Investigation into the Molar Feeding Ratio and Temperature Dependence on the Replacement Reaction between Platinum ions and Silver Nanoparticles

By

**Archimedes Stuk**

Submitted to the Department of Mechanical Engineering  
In Partial Fulfillment of the Requirements for the Degree of  
Bachelor of Science in Mechanical Engineering

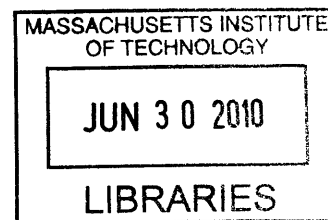
at the

Massachusetts Institute of Technology

June 2010

© 2010 Massachusetts Institute of Technology  
All rights reserved

**ARCHIVES**



Signature of Author.....

.....  
Department of Mechanical Engineering  
May 13, 2010

Certified By.....

.....  
Kimberly Hamad-Schifferli  
Assistant Professor of Mechanical Engineering  
Thesis Advisor

Accepted By.....

.....  
John H. Lienhard V  
Collins Professor of Mechanical Engineering  
Chairman, Undergraduate Thesis Committee

# **Investigation into the Molar Feeding Ratio and Temperature Dependence on the Replacement Reaction between Platinum ions and Silver Nanoparticles**

by

Archimedes Stuk

Submitted to the Department of Mechanical Engineering  
On May 13, 2010 in Partial Fulfillment of the Requirements for  
the Degree of Bachelor of Science in Mechanical Engineering

## **Abstract**

The deliberate structuring of bimetallic nanoparticles has useful applications in both fuel cell applications and biomedical research. This thesis studies the replacement reaction between platinum ions and silver nanoparticles, with the goal of synthesizing platinum-shelled silver nanoparticles. Specifically, the molar feeding ratio and the temperature dependence on the reaction were investigated. At low levels of supplied platinum, the nanoshells were only partially formed, but at a 1:1 molar ratio, non-uniform thickness nanoshells were formed with large amounts of silver on the surface. The temperature dependence showed increasingly thick shell formation; however, cyclic voltammetry measurements indicated the surface of the nanoparticles contained excessive levels of silver, deeming the particles inadequate for use as fuel cell catalysts. Through high temperature reactions, the surface plasmon resonance excitations peaks of the silver nanoparticles were shifted 100nm higher, pushing the peaks closer to the visible spectrum from the deep ultraviolet region.

Thesis Supervisor: Kimberly Hamad-Schifferli  
Title: Assistant Professor of Mechanical Engineering

## Table of Contents

<b>Chapter 1</b>	<b>Introduction</b> .....	5
<b>Chapter 2</b>	<b>Methods</b> .....	6
2.1	Silver nanoparticle synthesis.....	6
2.2	Molar ratio dependence.....	6
2.3	Temperature dependence.....	7
2.4	Characterization methods.....	7
2.4.1	UV-Vis Spectrometry .....	7
2.4.2	Transmission Electron Microscopy.....	8
2.4.3	X-Ray Diffraction.....	8
2.4.4	Cyclic Voltammetry.....	8
<b>Chapter 3</b>	<b>Results</b> .....	9
3.1	Starting materials.....	9
3.2	Molar Feeding Ratio dependence.....	9
3.3	Temperature dependence.....	13
3.4	Cyclic Voltammetry .....	17
<b>Chapter 4</b>	<b>Summary</b> .....	18
<b>Chapter 5</b>	<b>Further Research</b> .....	19
<b>References</b>	.....	20
<b>Appendix</b>	.....	21

## List of Figures

Figure 1	Ultraviolet Spectroscopy and X-Ray Diffraction Data, and TEM image of Silver Nanoparticles.....	9
Figure 2	Ultraviolet Spectroscopy of Molar Ratio Varied Platinum Silver Nanoparticles.....	10
Figure 3	TEM Imaging of Ag-Pt Nanoparticles Synthesized Using Varied Molar Ratios..	11
Figure 4	Ultraviolet Absorption Intensity degradation as a function of Molar Ratio.....	12
Figure 5	X-Ray Diffraction Data of Feeding Molar Ratio Dependent Ag-Pt synthesis.....	13
Figure 6	TEM Imaging of Temperature Dependent Ag-Pt Nanoparticle Synthesis.....	14
Figure 7	Ultraviolet Spectroscopy of Temperature Dependent Ag-Pt Synthesis.....	15
Figure 8	X-Ray Diffraction Data of Temperature Dependent Ag-Pt Synthesis.....	17
Figure 9	Comparison of Electrochemical Analysis of Ag-Pt Nanoparticles to Bulk Platinum Nanoparticles.....	18

## List of Tables

Table 1	Summary of Ag-Pt Molar Ratio Synthesis Properties.....	11
Table 2	Summary of Ag-Pt Temperature Synthesis Properties.....	16

## 1 Introduction

The high cost of catalysts used in conventional fuel cell systems poses an incredible challenge to the future of fuel cell development. Platinum nanoparticles and alloys with other metals are the most common catalysts for fuel cells [1,2]. Although there are many investigations into using non-platinum catalysts, platinum is the favored catalyst since it provides ample catalytic activity at low temperatures [3]. However, platinum catalysts often account for over half the system cost of common fuel cell designs due to the high price of the precious metal [4]. If the current amount of platinum per fuel cell is maintained, mainstream adoption of fuel cell technology would push platinum demand beyond worldwide supply, without factoring in other uses of platinum [5]. In order to achieve mainstream use of fuel cells, it is imperative to find methods to reduce the cost of current platinum catalysts, either by increasing the catalytic activity or reducing production costs.

The catalytic activity of metals is strongly dependent on the size and shape of the particles [6]. Smaller, spherical particles are preferred as they provide greater surface area for catalysis with respect to the particle volume. Nanoparticles, or particles between 1 and 100nm in size, can be made from a variety of materials and have been used for a broad range of applications such as drug delivery, cancer therapy, bioengineering, cosmetics, in addition to fuel cell applications. They have been of interest for applications because of their size dependent properties that differ from their bulk counterparts. Nanoparticles are commonly engineered in many shapes, ranging from simple spheres, cubes and cones, to more complicated architectures of tubes, hexagons, and bone-shapes [7]. Nanoparticles are ideal as catalysts in fuel cells since their surface area to volume ratio is favorably high, where about half of the atoms in a 2nm diameter particle are on the surface.

Still, it is possible to further increase the catalytic activity of a given amount of platinum than by reducing the particle size. In particular, control over composition could improve catalytic activity. Bimetallic nanoparticles, or particles comprised of two types of metal, have been synthesized out of many different types of metals for a plethora of applications. For use as a catalyst, platinum can be deposited on template nanoparticles of other materials, namely silver and gold, yielding an atomically thin platinum outer layer [8]. The thin platinum layer exhibits acceptable catalytic activity with only a fraction of the platinum used [9]. The advantage of using a silver core is that as a noble metal, it has low reactivity, but is still cheaper to purchase

and more plentiful in the environment than platinum or gold. Under the right conditions, the template material from the base nanoparticle can permeate the porous platinum layer enclosing it, yielding an empty nanoshell of porous platinum [8].

In this thesis, the synthesis of platinum-shelled silver nanoparticles is studied. The primary reaction in the synthesis requires a solution of chloroplatinic acid added to aqueous silver nanoparticles. Specifically, the paper reports on temperature dependence of the synthesis reaction from 0C-100C. Additionally, the molar ratio of precursors is examined to find the optimal level for platinum nanoshell synthesis. Section 2 will introduce the methodology behind the experiments. The results will be explained in section 3. Overall conclusions from the research will be made in Section 6. Recommendations for further research will be made in Section 7.

## 2 Methods

### 2.1 Silver Nanoparticle Synthesis

Silver nanoparticles were synthesized using a method adapted from Raj et al. [10]. Silver nitrate (99.998%), trisodium citrate (99%), and sodium borohydride were used as received from Sigma-Aldrich. Highly pure water with resistivity greater than 18.0 MV·cm was used throughout the experiment. A 50mL solution of  $10^{-3}$ M silver nitrate was prepared in a standard beaker which had been thoroughly cleaned beforehand. While vigorously mixing with a magnetic stir bar, a 1 mL solution of 1% trisodium citrate was added to the silver nitrate solution. Immediately after combining solutions, 2 mL of 0.1M sodium borohydride was added dropwise to the solution. The solution was left stirring for 1 hour at room temperature, yielding a gray-yellow colloid of silver nanoparticles.

### 2.2 Molar Feeding Ratio Dependence

The primary synthesis reaction is a reduction of chloroplatinic acid in the presence of silver nanoparticles. After the chloroplatinic acid is reduced, in order for all the silver to react with the free platinum ions, a standard molar ratio of 4:1 is necessary according the equation below.



Since the platinum forms an atomically thin shell around the silver nanoparticles, only the silver atoms on the surface of the nanoparticles interact with the platinum. The reaction was performed with the standard ratio modified by 1:1, 2:1, 5:1, and 10:1. The trial synthesis solutions were prepared in the proportions as follows: for the 1:1 standard ratio, 1 mole of silver was supplied for 1/4 mole of platinum, for the 2:1 standard ratio, 1 mole of silver was supplied for 1/8 mole platinum, for the 5:1, 1mole of silver for 1/20 mole of platinum, for the 10:1, 1 mole of silver for 1/40 mole of platinum. For each trial, 5 ml of the silver nanoparticle colloid was added to a small vial at room temperature. A solution of  $1.22 \times 10^{-3}$  M chloroplatinic acid ( $\text{H}_2\text{PtCl}_6$ ) was created with the combination of 5.01g solid chloroplatinic acid in 10mL of deionized water. The chloroplatinic acid solution was added dropwise to the silver nanoparticle solution under vigorous magnetic stirring in the amounts as follows: 1ml for the 1:1 reaction, 0.5ml for the 2:1 reaction, 0.2ml for the 5:1 reaction, and 0.1ml for the 10:1 reaction. The solutions were left stirring at room temperature for 1 hour.

## **2.3 Temperature Dependence**

Vials of 5ml of the silver nanoparticle colloid and 1ml of the  $1.22 \times 10^{-3}$  M chloroplatinic acid were prepared separately. A water bath was heated to 50°C on a hot plate. The vials of solution were placed in the water bath to acclimate for 10 minutes. The chloroplatinic acid was then added dropwise to the vial of silver nanoparticles under vigorous magnetic stirring. The solution was left stirring in the water bath for 1 hour. The temperature dependence experiments were further performed at 75°C and 100°C. For a 0°C trial, an ice bath was used instead of a hot water bath.

## **2.4 Characterization Methods**

### ***2.4.1 UV-Vis Spectrometry***

All finished samples were submitted to ultraviolet spectrometry using a Cary 300 UV-Vis Spectrophotometer. Polymethacrylate fluorimeter cuvetts were cleaned and loaded with deionized water for baseline subtraction. The UV-Vis spectra of those samples were recorded at the wavelength range from 200nm to 900 nm.

#### ***2.4.2 Transmission Electron Microscopy (TEM)***

The nanoparticles for TEM study were collected by centrifuge at 6000 rpm three times and then re-dispersed into deionized water. A drop (~2  $\mu\text{L}$ ) was placed onto an amorphous carbon coated copper grid and allowed to dry overnight. The samples were investigated using a JEOL 200CX transmission electron microscope at 200 kV. Particle size was determined by first using the GNU Image Manipulation Program to sharpen the TEM images and ImageJ to analyze size and aspect ratio.

#### ***2.4.3 X-Ray Diffraction (XRD)***

The nanoparticle powders were collected by centrifuging for 10 minutes at 8000 rpm and then re-dispersed in 0.5 mL deionized water. The concentrated colloid solutions were then dropped onto glass slices to form a thin film within an area  $1\text{cm} \times 1\text{cm}$ . The XRD patterns of these samples were recorded on a Panalytical X'pert Pro with Cu Ka radiation ( $\lambda=1.5418 \text{ \AA}$ ).

#### ***2.4.4 Cyclic Voltammetry (CV)***

The sample for CV measurement was collected by centrifuging at 8000 rpm for 10 min. The collected wet powders were re-dispersed in deionized water by sonication. The centrifuge step was repeated for three times for washing powders and removing impurities such as sodium citrate. The wet powder was finally dispersed in 0.1 mL deionized water to form a concentrated colloid. The colloid solution was then dropped onto a glass carbon electrode and allowed to dry overnight. For comparison, pure Pt nanoparticles were also loaded onto the electrode for electrochemical measurement. The electrochemical measurements were performed on a Pine Instrument. The CV curves were recorded in an Ar-saturated 0.5 M  $\text{H}_2\text{SO}_4$  electrolyte with a scan rate of 50 mV/s at the potential window of ~0.04-1.7 V (vs RHE). A Pt wire and a saturated calomel electrode (SCE, Analytical Sensor, Inc.) were used as the counter electrode and the reference electrode, respectively.



### 3 Results

#### 3.1 Starting Materials (Silver nanoparticles)

The UV-Vis shows that unaltered silver nanoparticles have a strong, narrow peak at 378nm, as seen in Figure 1 (dashed blue). The silver nanoparticles also show a trough at 312nm. From the TEM image, the silver nanoparticles are non-spherical, amorphous shapes. The particles are on average  $16.7 \pm 7.0$  nm in diameter. The particles exhibit a main peak on the XRD at  $38^\circ$ , with the next major peak at  $44^\circ$ .

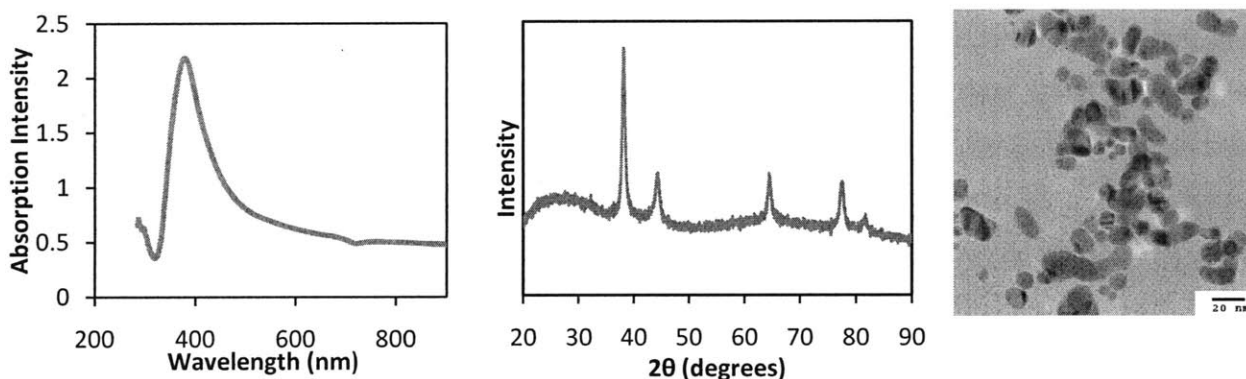
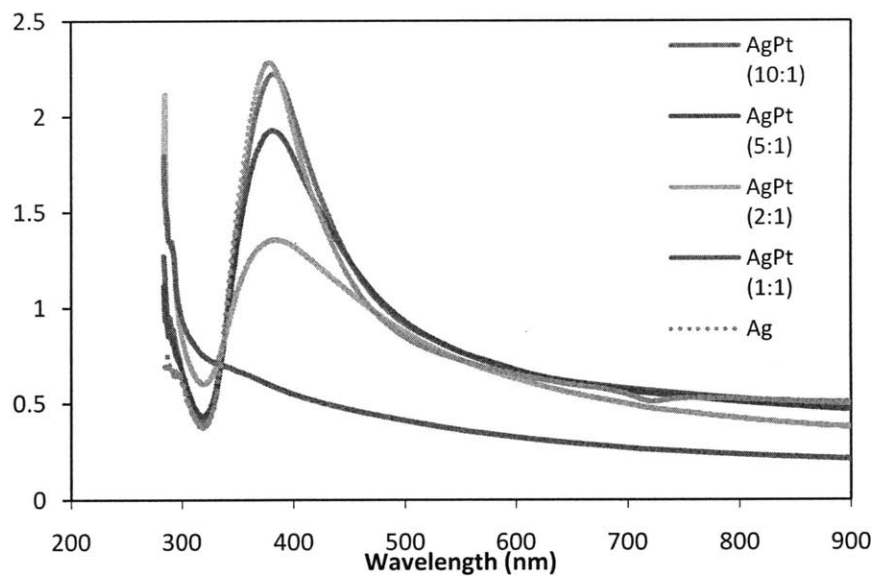


Figure 1: Ultraviolet Spectroscopy, X-Ray Diffraction Data, and TEM image of Silver Nanoparticles.

#### 3.2 Molar Ratio Dependence

The molar ratio of silver to platinum in the replacement reaction is influential on the optical properties and the morphologies of particle products. It is known that silver nanoparticles exhibit remarkable surface plasmon resonance in the ultraviolet range, while platinum does not show such an optical property. Therefore, the UV-Vis absorption spectrum is a direct technique to study the as-prepared Ag-Pt colloids. A summary of important data from the trials can be found in Table 1. However, it is commonly known that platinum shows known surface plasmon resonance peaks from 200nm-900nm. The 10:1 Ag-Pt particles (Figure 2, purple) show only a slight decrease of this peak (4%), indicating that little platinum has coated the silver nanoparticle surface to block the plasmon resonance of silver. The 10:1 reaction has surface plasmon resonance almost identical to that of the unaltered silver nanoparticles, indicating the 10:1 reaction is undoubtedly starved of platinum. The peak position shifts to 382nm. From the TEM image in Figure 3a, the 10:1 synthesis shows small platinum particles attached to only some of

the silver nanoparticles, though no particles have complete coverage, which supports the absorption data. The silver nanoparticles have a diameter  $16.9 \pm 7.8$  nm, while the platinum nanoparticles appear to be 1nm-2nm in diameter. Large particles have aggregated from smaller silver particles, a phenomenon which was not present in the pure silver but is in the other molar ratio samples.



**Figure 2: Ultraviolet Spectroscopy of Molar Ratio Varied Platinum Silver Nanoparticles.**

The 5:1 reaction shows a 17% intensity drop in the peak of surface plasmon resonance (Figure 2, maroon). This moderate reduction of surface plasmon shows that the silver nanoparticles are partially covered with platinum, either covering portions of all particles, covering a portion of the particles completely, or a combination of the two. The peak position shifts to 381nm. The TEM imaging (Figure 3b) shows increased coating of platinum on silver nanoparticles. The platinum coats some silver particles entirely, forming thin, but complete shells around them. Still, many particles are left uncoated. It is possible that platinum layer growth outpaces platinum nucleation, meaning the free platinum after the reduction of the chloroplatinic acid has an affinity to bind to other platinum that has already attached to a silver particle, than begin nucleation on a barren silver particle. There are some very large silver particles present with diameters in excess of 40nm, assumed to have aggregated from smaller silver particles. There are less of these large particles than in the 10:1 sample. Though some of

the nanoparticles show promising shell formation, the persistence of unaltered silver nanoparticles deems the 5:1 molar ratio inadequate.

**Table 1: Summary of Ag-Pt Molar Ratio Synthesis Properties.**

Nanoparticle	Size (nm)	Peak Absorption (% of silver NP)	Peak Location (nm)	Nanoshell (Y/N/Partial)
Silver nanoparticle	16.7±7.0	100	378	No
25C 10:1 Reaction	16.9±7.8	96	382	No
25C 5:1 Reaction	17.3±9.7	83	381	Partial
25C 2:1 Reaction	16.8±8.2	59	385	Partial
25C 1:1 Reaction	17.5±7.5	24	None	Yes

The 2:1 Ag-Pt colloid exhibits a 41% drop in surface plasmon resonance compared to pure Ag (Figure 2, green). The TEM imagery shows a large region of silver nanoparticles covered by platinum particles, yet still there are large clumps silver nanoparticles with no platinum nucleation (Figure 3c). Interestingly, both particles as larger than 50nm in diameter as well as particles less than 8nm in diameter that have formed thick shells. From the TEM, though, it is unclear to what degree these shells are pure platinum. The 1:1 Ag-Pt colloid shows a 76% reduction of surface plasmon resonance at the peak position (Figure 2, dark blue). Actually,

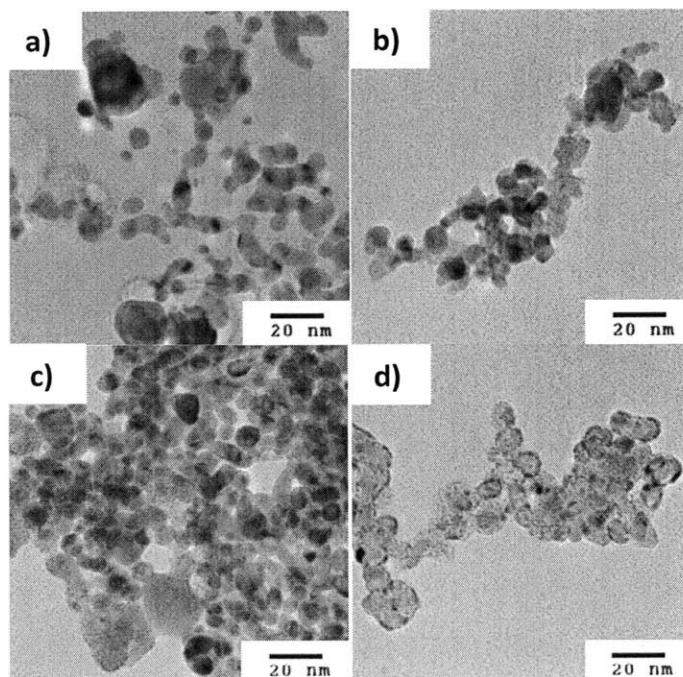


**Figure 3: TEM Imaging of Ag-Pt Nanoparticles Synthesized Using Varied Molar Ratios.** The particles were synthesized using a ratio of silver to platinum of a.) 10:1, b.) 5:1, c.) 2:1, and d.) 1:1 at room temperature.

there is no visible peak exhibited, the surface plasmon resonance profile shows the smooth peakless curve indicative of a pure platinum surface. The trough exhibited by the silver nanoparticles has been eliminated, further indicating the platinum has covered all the surface of the silver nanoparticles. The dark rings around the silver nanoparticles reveal a coating of the nanoparticles not only on the plane visible to the TEM electron beam, but also around the sides of the particles (Figure 3d). All particles appear to have formed nanoshells, no unaltered silver particles are visible. The nanoparticles appear to have the most consistent size of any trial except the original silver particles, at  $17.5 \pm 7.5$  nm (Figure 3d).

The degradation of the surface plasmon resonance peak as precursor molar ratio increases shows a strong, trend across all samples. Figure 4 shows the linear reduction of the plasmon resonance peak intensity as the precursor ratio increases. This result is important because eliminating this peak indicates that the surface of nanoparticles was covered by Pt and the coverage of Pt can be fine tuned by varying the feeding ratio of precursors. It is significant to note that the position of the peak remained within a few nanometers for all trials, indicating that the particles did not aggregate.

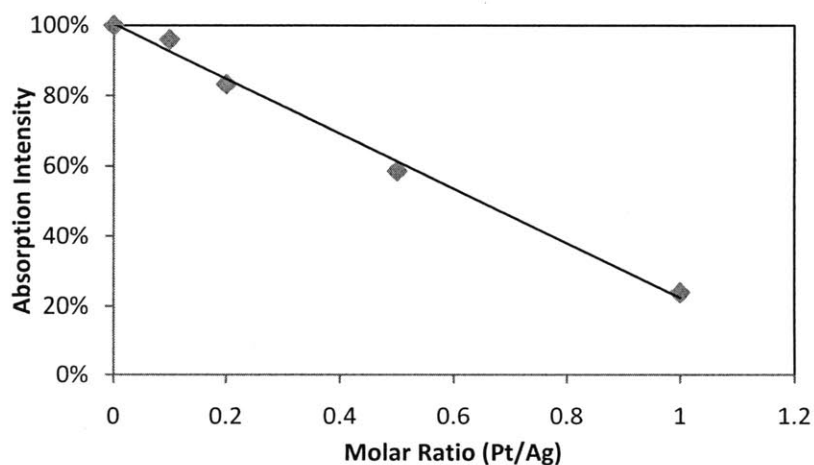


**Figure 4: Ultraviolet Absorption Intensity degradation as a function of Molar Ratio.**

To identify the crystal phases of produced Ag-Pt nanoparticles, their X-ray diffraction patterns were recorded. The X-ray diffraction peaks were compared to those of standards: bulk platinum (Figure 5, small gray dots), bulk silver (large red dashes), and silver chloride (small

blue dashes). The X-ray diffraction patterns in Figure 5 show a reduction of silver in the sample as the amount of platinum in the feeding ratio increases. There is significant presence of silver in all the samples, but it has been reduced to only 11% of its initial peak in the 1:1 reaction. Only in the 1:1 reaction is there strong notes of platinum appearing in the X-ray diffraction pattern at 47°. The platinum peak, though, is not as strong as the silver peak, indicating the surface is not pure platinum, as hoped. There are peaks of silver chloride present in the samples, increasing in magnitude as more platinum is added to the molar ratio. There are notes of silver chloride present in the samples, increasing in magnitude as more platinum is added to the molar ratio. The silver chloride, as a by-product, was produced by Ag and Cl ions. Ag ions came from the replacement reaction between Ag nanoparticles and Pt ions, while Cl ions came from the precursor of Pt, chloroplatinic acid.

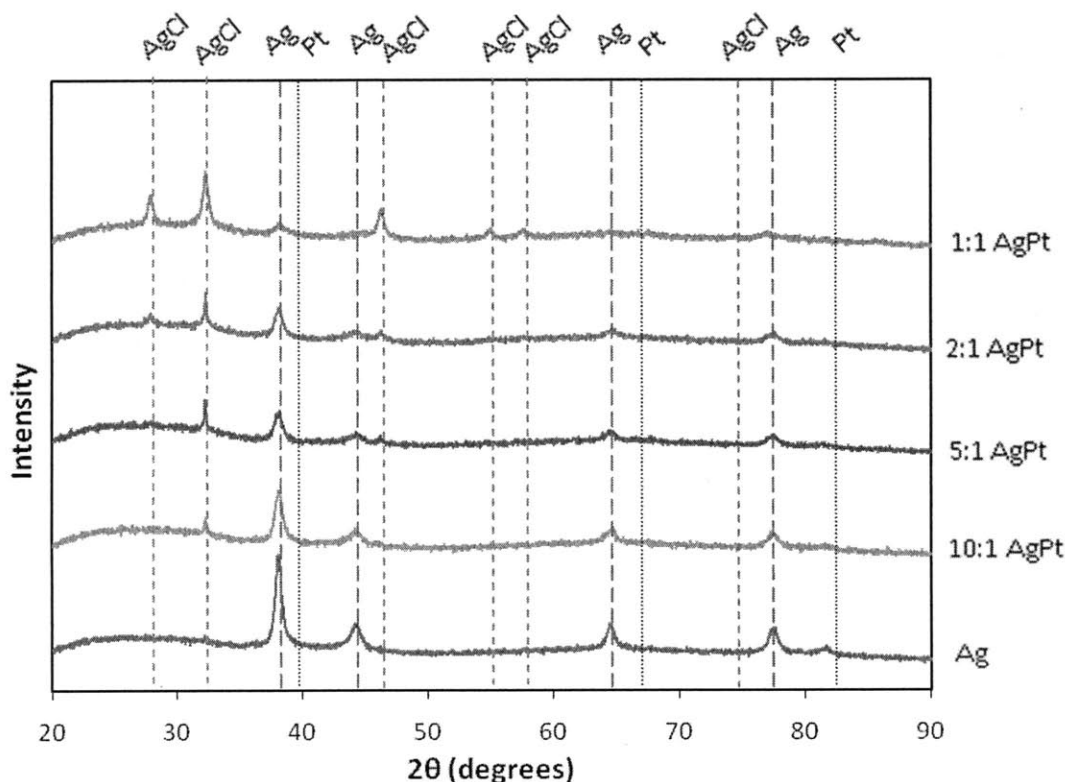
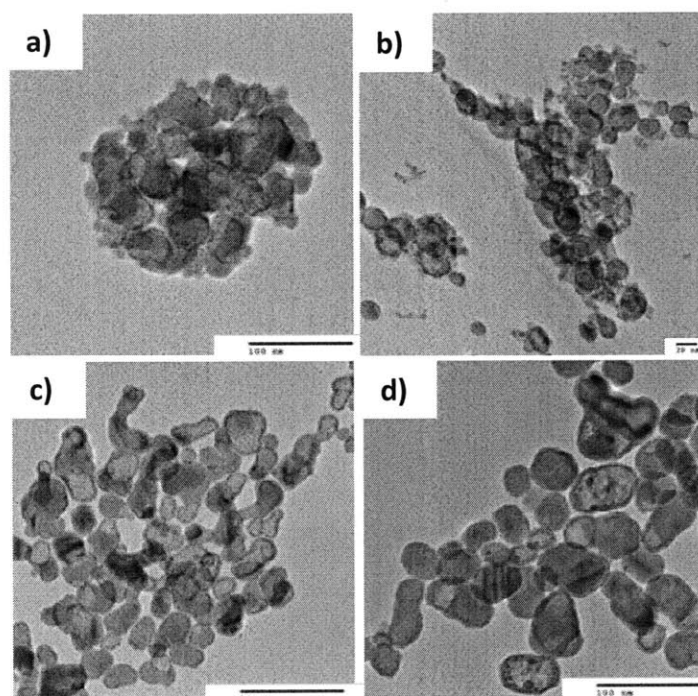


Figure 5: X-Ray Diffraction Data of Feeding Molar Ratio Dependent Ag-Pt Synthesis.

### 3.2 Temperature Dependence

The temperature of the synthesis reaction plays a major role in nanoshell thickness, size of the nanoparticles produced, and the optical properties of the nanoparticles. A summary of

important data from the trials can be found in Table 2. At 0°C, the reaction is hindered due to the low kinetics of the reaction between Ag nanoparticles and Pt ions. The TEM images in Figure 6 show complete platinum shells on many particles, however not all particles are covered with platinum. There are some small silver nanoparticles (<10nm) that have remained independent and uncoated with platinum. The low kinetic energy from the low reaction temperature causes the silver nanoparticles to show a low affinity for forming larger silver particles. Still, the ultraviolet spectroscopy shows a peak shift to 470nm, indicative of larger silver nanoparticles forming, but with a partial Pt coating (Figure 7, light blue). The absorption intensity at the peak has been greatly reduced, 73% less than the peak of pure silver nanoparticles. The TEM imagery shows many of these large particles with substantially thick shells of 1-2nm (Figure 6a).



**Figure 6: TEM Imaging of Temperature Dependent Ag-Pt Nanoparticle Synthesis. Silver nanoparticles were reduced with chloroplatinic acid at a) 0°C, b) 50°C, c) 75°C, and d) 100C.**

The 25°C synthesis leads to the purest platinum shells created as no large surface plasmon resonance peaks are detected (Figure 7, purple). A slight peak around 380nm is likely from a few original silver nanoparticles remaining. The TEM image and size counting show a highly variable size for these particles, some <10nm particles exist as well as those of 40nm

(Figure 3d). Some of these particles have thick platinum-silver shells, while some have only thin shells, with no dark ring of platinum around the silver nanoparticle.

The 50°C reaction benefits from higher kinetic energy in that the platinum shells are more uniform in thickness across the sample. Some particles appear to be hollow shells, as the higher kinetic energy may have allowed the produced Ag ions to be reduced back to Ag again, passing through holes in the platinum coatings (Figure 6b). A broad peak appears on the UV-Vis spectrum, beginning at 390nm and ending around 420nm (Figure 7, green). This wide peak

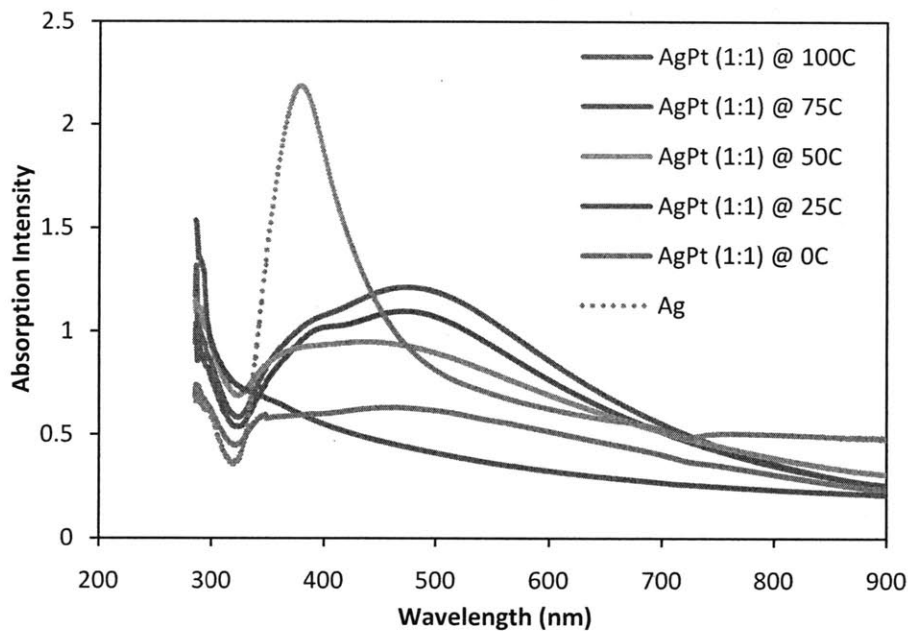


**Figure 7: Ultraviolet Spectroscopy of Temperature Dependent Ag-Pt Synthesis.**

may be due to either formation of larger silver nanoparticles or silver coating the outside of the platinum shell, or both. Since the surface plasmon resonance of silver depends on the nanoparticle size and morphology, we can assume that larger silver nanoparticles exist than before the synthesis. TEM imagery in Figure 6b shows almost all nanoparticles with distinct shells of platinum around them, so the wide peak cannot be from the combining of two pure silver particles. This wide peak may imply silver particles from the hollow cores are beginning to coat the platinum shells, or that an agglomeration of alloyed silver and platinum particles is forming when two smaller, platinum shelled particles fuse into a single larger particle.

**Table 2: Summary of Ag-Pt Temperature Synthesis Properties.**

<b>Nanoparticle</b>	<b>Size (nm)</b>	<b>Peak Absorption (% of silver NP)</b>	<b>Peak Location (nm)</b>	<b>Nanoshell (y/n/partial)</b>
0C 1:1 Reaction	16.5 ±7.4	28	470	Yes
25C 1:1 Reaction	17.5±7.5	24	None	Yes
50C 1:1 Reaction	17.4±6.7	40	390-420	Yes
75C 2:1 Reaction	18.5±7.9	46	390,480	Yes
100C 1:1 Reaction	20.6±9.4	50	482	Yes

The 75°C synthesis particles show the strong shell formation consistent across all particles. The particle size has increased to 18.5± 7.9nm. The particles show very light centers on the TEM, implying that the particle cores may be hollow (Figure 6c). A double peak has appeared on the ultraviolet spectrometry, one peak around 390nm which is considerably close to the original silver nanoparticles' peak and one at 480nm (Figure 7, red). The second broad peak probably is due to the Ag surface feature, which is formed by reduction of produced Ag ions back onto the Pt shell and thus a Pt/Ag nanoshell is formed.

The 100°C synthesis particles are and quite similar to the 75°C particles. The particles are quite large now, averaging 20.6± 9.4nm. The double peak exhibited by 75 °C in the UV-Vis spectrum has coalesced more into a single peak at 482nm, as the smaller peak around 390nm has almost disappeared (Figure 7, dark blue). Additionally, the TEM shows thick shells on these nanoparticles (Figure 6d), similar to the 50°C and 75°C particles, as the silver ions are reduced onto the Pt shells, the free silver attaches to the outside of the platinum shells. In the 100°C case, a large amount of silver has attached to the outside of the platinum shell, creating perhaps a double shelled particle, an inner shell of platinum and an outer shell of silver, which actually is an interesting nanostructure for optical-property-based applications.

From the X-ray diffraction patterns (Figure 8), silver chloride dominates the temperature dependent samples. The size of the silver chloride peak with respect to the silver peak increases with temperature from 0°C to 75°C. At 100°C, the high temperature breaks down the silver chloride, as the silver peak is 32% the size of the silver chloride peak, the highest of all the samples. The platinum peaks remain fairly small across all samples, indicating lower platinum on the surface than anticipated. These results show that varying the reaction temperature can strongly affect the morphology of the AgPt particles.



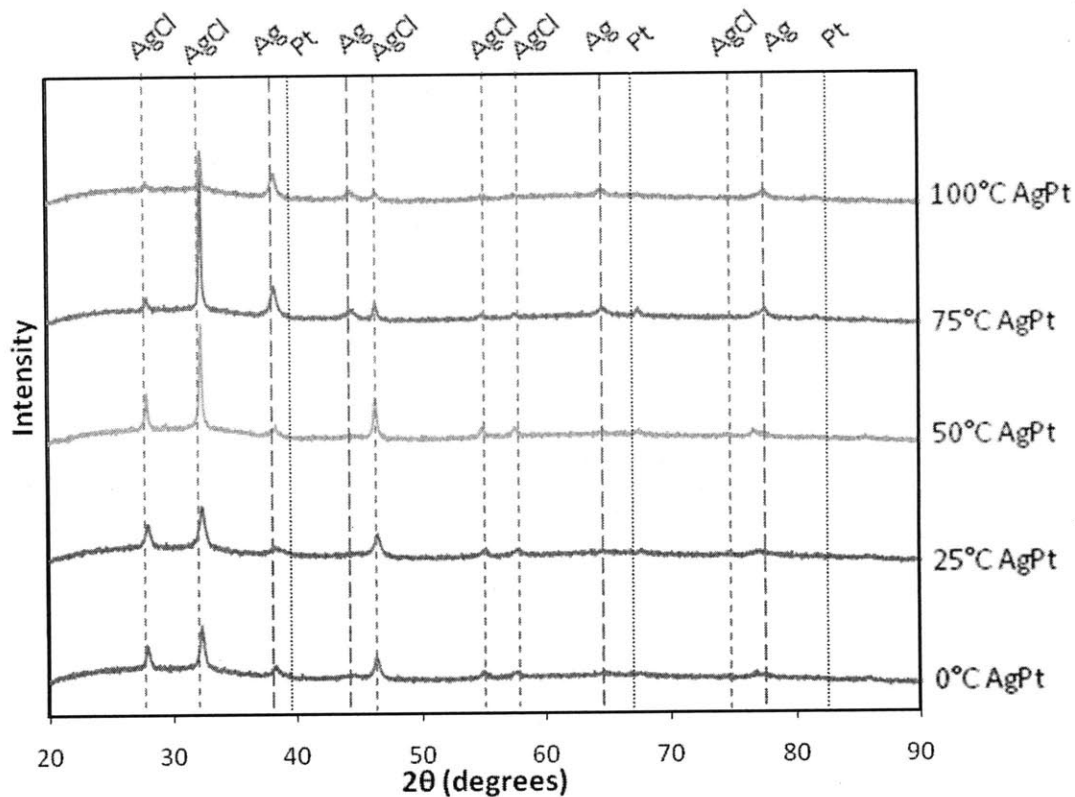
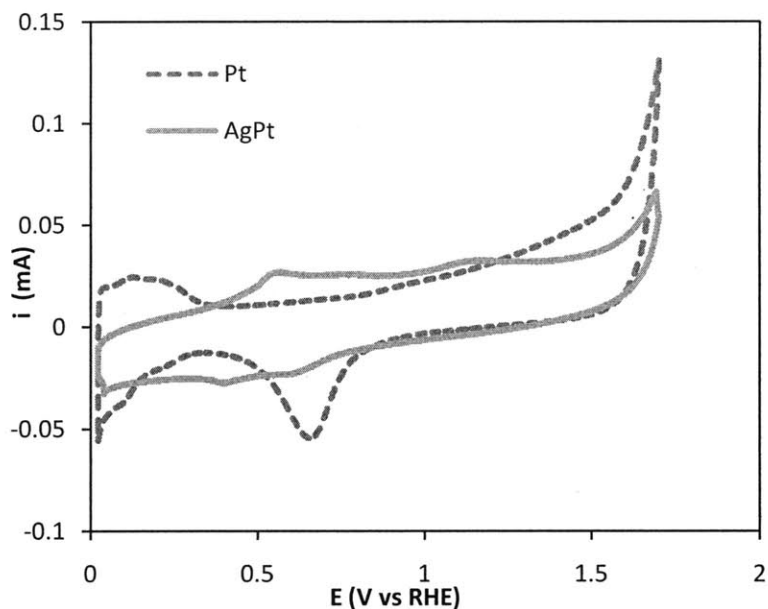


Figure 8: X-Ray Diffraction Data of Temperature Dependent Ag-Pt Synthesis.

### 3.3 Cyclic Voltammetry

The cyclic voltammetry was used to study the surface chemistry. The UV-Vis absorption spectrum shows optical information of particles' surface chemistry, while the electrochemical signal may give a more insight view on the surface chemistry of nanoparticles. Electrochemical analysis was conducted on the 1:1 molar ratio particles synthesized at 25°C since the UV-Vis spectrum indicated the sample had the lowest amount of silver on the nanoparticle surfaces. The silver-platinum nanoshells analyzed have only very small amount of platinum on the surface, according to the comparison with pure platinum nanoparticles in Figure 9. The analysis of silver-platinum shells shows peaks in the regions where silver oxidizes and reduces, but only weak feature of Pt redox peaks. Additionally, the silver-platinum nanoshells exhibit almost no typical hydrogen evolution on Pt surface. Comparatively, the pure platinum particles show a significant peaks from 0.0 to 0.3 V (vs RHE), the region of hydrogen adsorption and de-absorption.

This test indicates that the surface of the silver-platinum nanoparticles is predominantly silver, though some small amounts of platinum exist. The presence of silver on the surface of the particles diminishes their practical use as catalysts in hydrogen fuel cells. However, the electrochemical analysis definitively shows the persistence of silver on the nanoparticles' surfaces, despite UV-Vis spectrophotometer readings indicating the opposite.



**Figure 9: Comparison of Electrochemical Analysis of Ag-Pt Nanoparticles to Bulk Platinum Nanoparticles.**

#### 4 Summary

The synthesis of platinum-shelled silver nanoparticles is a complicated science. While this study has by no means perfected the synthesis methods, it has shed insight into a better process. The synthesis is highly dependent on the molar ratio of the silver nanoparticles and the platinum supplied by the chloroplatinic acid. While some nanoshells were formed with low levels of platinum, the 10:1, 5:1, and 2:1 molar ratios yielded inadequate samples with some silver particles only partially covered with platinum, while many particles had no platinum coating at all. The 1:1 molar ratio produced a nanoshell coating on all particles in the sample, however, the shells formed had non-uniform in thickness across the sample and had large amounts of silver present on the surface.

The temperature dependence of platinum-shelled particle synthesis was thoroughly examined. At low temperatures (0°C), the low reaction kinetics impeded growth of the particles, while still forming distinct nanoshells. At high temperatures, from 50°C-100°C, the reaction produced increasingly thicker shells and increasingly larger particles as particle size almost doubled during the 100°C synthesis. At these temperatures, the high reaction activity created a second reduction of the Ag ions to Ag, with a shell of silver coating the platinum shells.

The silver-platinum nanoparticles synthesized here cannot be used for catalysis in fuel cells due to the high presence of silver on the surface of the nanoshells. The mechanism for coating did not behave as expected, with no pure platinum shells formed around silver cores. While UV-Vis spectrometry and TEM imaging indicated that the silver-platinum shells would be formed as expected, the electrochemical measurement proves that the surface composition of particles is the critical quality of good catalysts. The synthesis of bimetallic nanoshells is a more complicated reaction than a simply choosing two elements and mixing them. It is important to take strong consideration into how the by-products of the synthesis reaction will behave, as significant presence of silver chloride has interfered with this study's results.

However, through high temperature reactions, the surface Plasmon resonance excitations peaks of the silver nanoparticles were shifted almost 100nm higher, pushing the peaks more close to visible spectrum from the deep ultraviolet region. This ability to manipulate the optical properties of silver nanoparticles is very interesting. It indicates a technique to control the optical properties of noble metal nanoparticles by changing their morphology and composition. By this primary study, the well-controlled nanostructures with desired optical properties can be expected in future studies, which will be very appealing to biology related applications.

## **5 Further Research**

While a substantial amount was learned about bimetallic silver-platinum particles synthesis from this study, it has more importantly brought forth new areas of research. First, the effect of even higher temperature synthesis should be investigated. High temperature synthesis produced a 100 nm red-shift in the surface plasmon resonance peak, perhaps synthesis at a higher temperature could push this peak to an even higher wavelength. It must be noted though that these tests would need to use a different solvent as a test using water can only reach 100°C.

Instead of a higher temperature synthesis, it different core nanoparticle could be used. Gold nanoparticles, with a surface plasmon resonance peak around 530nm, would be ideal to use, for if 100 nm or even more red-shift was achieved, the peak would be in the 600-700 nm range, a very useful wavelength for photothermal therapy and optical imaging.

## 6 References

- [1] Gonzalez-Huerta, R.G., Chavez-Carvayar, J.A., Solorza-Feria, O., “Electrocatalysis of Oxygen Reduction on Carbon Supported Ru-Based Catalysts in A Polymer Electrolyte Fuel Cell”, *Journal of Power Sources*, 153:11–17 (2006).
- [2] Larminie, J., Dicks, A., “Fuel Cell Systems Explained”, John Wiley & Sons, New York, 66-69 (2000).
- [3] Verde-Gomez, Y., Alonso-Nunez, G., Cervantes, F., Keer, A., “Aqueous Solution Reaction to Synthesize Ammonium Hexachloroplatinate and Its Crystallographic and Thermogravimetric Characterization”, *Materials Letters*, 57: 4667-4672 (2003).
- [4] Spendelow, Jacob “Fuel Cell Systems Cost” US Department of Energy, 2 (2009)
- [5] Anderson, Arlene, “Platinum Availability and Economics for PEMFC Commercialization” US Department of Energy, 3-5 (2003)
- [6] Wang, H., Sun, X., Ye, Y., Qiu, S., “Radiation Induced Synthesis of Pt Nanoparticles Supported on Carbon Nanotubes”, *Journal of Power Sources*, 161:839-842 (2006).
- [7] Sun, Yugang, Xia, Younan, “Shape-Controlled Synthesis of Gold and Silver Nanoparticles”, *Science* 298:2176-2179 (2002)
- [8] Zeis, R., Mathur, A., Fritz, G., Lee, J., Erlebacher, J., “Platinum-plated nanoporous gold: An efficient, low Pt loading electrocatalyst for PEM fuel cells”, *Journal of Power Sources*, 165:65-72 (2007)
- [9] Yoo, S.-H., Park S., “Platinum-Coated, Nanoporous Gold Nanorod Arrays: Synthesis and Characterization”, *Advanced Materials*, 1912:1612-1615 (2007)
- [10] Raj, C. R., Ohsaka, T., “Electroanalysis of Ascorbate and dopamine at a gold electrode modified with a positively charged self-assembled monolayer”, *Journal of Electroanalytical Chemistry*, 496:44-50 (2001)
- [11] Schmid, K., Riediker, M., “Use of Nanoparticles in Swiss Industry: A Targeted Survey”, *Environmental Science and Technology*, 42: 2253-2260 (2008)

# Appendix

## A.1 Additional TEM Imagery

